Nanoscale

Cite this: *Nanoscale*, 2011, **3**, 3291

www.rsc.org/nanoscale

PAPER

Cellular uptake, evolution, and excretion of silica nanoparticles in human cells†

Zhiqin Chu,[a] Yuanjie Huang,[a] Qian Tao[b] and Quan Li*[a]

Received 15th February 2011, Accepted 20th May 2011
DOI: 10.1039/c1nr10499c

A systematic study on the interaction of silica nanoparticles (NPs) with human cells has been carried out in the present work. Endocytosis and exocytosis are identified as major pathways for NPs entering, and exiting the cells, respectively. Most of the NPs are found to be enclosed in membrane bounded organelles, which are fairly stable (against rupture) as very few NPs are released into the cytoplasm. The nanoparticle–cell interaction is a dynamic process, and the amount of NPs inside the cells is affected by both the amount and morphology (degree of aggregation) of NPs in the medium. These interaction characteristics determine the low cytotoxicity of SiO_2 NPs at low feeding concentration.

Introduction

Nanometre-sized materials with unique physiochemical properties suggest a number of advantages, such as improved bioavailability and easy tracking of drugs, when they are used in various bio-medical applications ranging from diagnostics to therapeutics.[1–4] In many of these applications, the nanomaterials are introduced to cells either as drugs (and drug carriers) or imaging agents. Consequently, how they interact with the cells, in particular, how they enter the cells, evolve inside the cells, and eventually how they are excreted out of the cells are the prerequisite information one needs to obtain before any further development of these nanomaterials for desired biomedical applications.

The interaction of cells with several different nanoparticle (NP) systems have been investigated in the literature, including Au,[5–7] SiO_2,[8–13] Fe_2O_3,[14] ZnO,[15] TiO_2,[15] some quantum dots such as CdSe and CdTe, CdS,[16–18] carbon nanotubes,[19] fullerene,[20] and polymeric nanoparticles (NPs).[21] Generally speaking, most of the NPs are found to enter the cells *via* endocytosis process during incubation. The endocytosed NPs are normally found in membrane bound organelles in the cytoplasm,[22] although bare NPs in the cytoplasm or other organelles such as nucleus[10] and mitochondria[23] are occasionally reported. Nevertheless, the mechanism behind the NPs evolution inside the cells and how NPs could enter the specific organelles is seldom discussed. Excretion of NPs from the cell is generally realized through lysosomal secretion,[5,24,25] while such processes can last from 0.5 to 48 hours according to different reports.[5,23]

Evaluation of the cytotoxicity of NPs is normally carried out *in vitro* using various colorimetric assays.[26] However, the colorimetric assay based methods only give the final stage judgement of the cytotoxicity. Even for the colorimetric assay experiments themselves, it seems that a number of parameters including the particle concentration, incubation duration, cell line type and evaluating standard would affect the toxicological results. In this sense, direct judgement of the biocompatibility of the NPs cannot be made from such cytotoxicity measurement alone.

Among different nanomaterials, silica NPs hold great practical application potential in the emerging nano-biotechnology, due to their hydrophilicity, stability in physiological environment, ease of production and relatively low cost. On the one hand, amorphous silica NPs are commonly considered as biocompatible mainly based on their toxic effect studied *in vitro* (mainly using colorimetric assay).[11,13] However, the claim of obvious cytotoxicity of the amorphous SiO_2 NPs is also found in the literature, particularly at high NPs dose and/or elongated cell–particle incubation duration.[8,9,12] It has been identified that once they enter the cells, most of them are located in membrane bounded organelles in the cytoplasm,[27] although reports on their entering the nucleus also exist.[10] Nevertheless, how these particles evolve inside the cells before their excretion is less discussed, although such information provides fundamental guidance in their design for practical drug/imaging applications. Despite the lack of detailed understanding on their interaction with the cells, much effort has already been devoted to the chemical development of amorphous silica NPs into drug[2,4]/DNA[3] carriers for various therapeutics, and as imaging agents.[1] On the other hand, crystalline silica NPs are often reported as carcinogens,[28] while the

[a]*Department of Physics, The Chinese University of Hong Kong, Shatin, New Territory, Hong Kong. E-mail: liquan@phy.cuhk.edu.hk*
[b]*Department of Clinical Oncology, Prince of Wales Hospital, The Chinese University of Hong Kong, Shatin, New Territory, Hong Kong*

† Electronic supplementary information (ESI) available: Low magnification TEM image of 400 nm amorphous silica NPs; TEM images depicting the evolution process of 50 nm silica NPs inside cells; Confocal microscopy images showing the interaction of silica NPs with cells; ζ potential of NPs in dispersion with different pH value; MTT results of H1299 and NE083 cells incubated with 400 nm and 10–20 nm amorphous silica NPs and light microscopy images of H1299 cells treated with 50 nm silica NPs. See DOI: 10.1039/c1nr10499c

evolution of these NPs inside the cell (in comparison with the amorphous counterparts) and the exact mechanism of cancer-causing remain arguable.

In the present study, we have systematically studied the interaction between SiO_2 NPs and human cells. In particular, we have investigated the uptake, sub-cellular distribution, evolution and excretion of SiO_2 NPs of different crystallinity for both normal and carcinoma cell lines. As crystalline SiO_2 NPs have been suggested as carcinogens for the respiratory system,[28] we have selected two cell lines including H1299 human lung carcinoma cell and NE083 human esophageal epithelial cell for such study (several other cell lines are also tested to make parallel comparison). Parameters affecting the NP–cell interaction have been studied, including, the NP crystallinity and the medium type (with/without serum). At the same time, the cytotoxicity of all silica NPs presented in this study has been evaluated by tetrazolium reduction (MTT) as functions of NP concentration in the medium and the incubation duration. The general uptake and excretion of the NP by different cells are discussed, and the interaction of NP with the cells before their excretion is elaborated based on the transmission electron microscopy (TEM) and confocal microscopy studies. Findings from this research give a clearer understanding on the NP–cell interactions, suggesting the potential of using silica NPs for various biomedical applications.

Results and discussion

1. Characterizations of the silica NPs

Fig. 1a shows a low magnification TEM image of the 50 nm silica NPs (synthesized by Stober's method) as an example. These amorphous NPs are spherical in shape, and their size distribution is quite narrow (Fig. 1a). As a comparison, the purchased amorphous NPs have smaller diameters (labeled as 10–20 nm by the manufacturer). Nevertheless, particle aggregation is severe (Fig. 1b). The shapes of the crystalline silica NPs appear to be irregular, and a size ranging from several tens to hundreds of nanometres after centrifugation can be clearly observed in Fig. 1c.

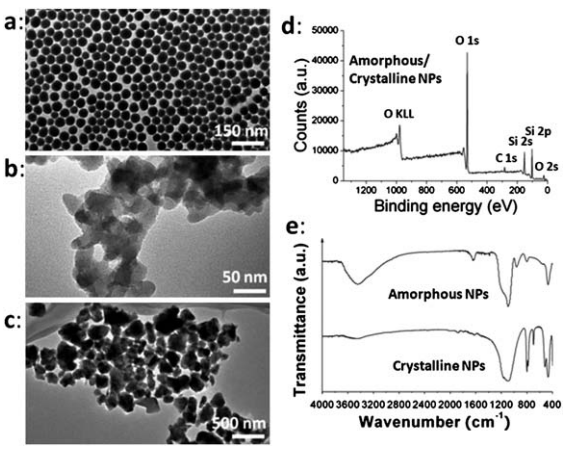

Fig. 1 Low magnification TEM images of (a) synthesized amorphous silica NPs (~50 nm in diameter); (b) purchased amorphous silica NPs (10–20 nm in diameter); and (c) purchased crystalline silica particles after centrifugation (tens to hundreds of nm in diameter); (d) typical XPS spectrum taken from silica NPs sample; (e) FTIR spectra taken from the amorphous and crystalline silica NPs.

Similar chemical composition of all silica NPs adopted in the present study has been suggested by the XPS study of these samples. Fig. 1d gives a representative XPS survey scan taken from one of the amorphous silica NPs. Only Si and O signals are detected. The carbon signal originates from the hydrocarbon contamination on the sample surfaces.

FTIR measurements of all the amorphous NPs samples suggest their similar surface chemical characteristics (representative data shown in the top curve in Fig. 1e). The four peaks (1085 cm^{-1}, 944 cm^{-1}, 802 cm^{-1}, 464 cm^{-1}) in the low wavenumber range can be ascribed to different vibrational modes of Si–O bonds, while the two other peaks at 1640 and 3440 cm^{-1} originate from the adsorbed water molecules, and O–H bonds of silanols, respectively. The FTIR spectrum taken from the crystalline NPs is consistent with the standard data of α-quartz,[29] which is characterized by its fingerprints located in the low wavenumber range (below 1085 cm^{-1}). A distinct difference between the amorphous and crystalline sample could be the abundance of –OH on the amorphous sample surfaces.

In order to determine the proper NPs concentration that will be used to feed the cell, DLS experiments have been carried out and the experimental results from two selected NPs concentrations are shown in Table 1. In DLS experiments, we measure the intensity–intensity time correlation function $G^2(\tau)$, from which the hydrodynamic radius (R_h) is deducted, revealing the extent of NPs aggregation in the solution.[30]

Table 1 shows the R_h of 50 nm amorphous silica NPs in PBS buffer at 10 μg ml^{-1} and 100 μg ml^{-1} as a function of time. At 10 μg ml^{-1} NPs concentration, the R_h of NPs in solutions does not change significantly with time. As a comparison, at 100 μg ml^{-1} NPs concentration, two R_h values can be identified immediately after the NPs are added to the solution, and the values keep changing as a function of time. This suggests that aggregation of NPs occurs significantly. We therefore select 10 μg ml^{-1} as the NPs concentration, at which value reasonable dispersion of NPs can be maintained for elongated durations.

2. Cellular uptake of the silica NPs

2.1 General description of the NP uptake and excretion process. The general process of NP uptake and excretion are rather similar for all NPs and cell lines selected. Here we illustrate the general picture using the 50 nm amorphous NPs and H1299

Table 1 Dynamic light scattering (DLS) results of 50 nm silica NPs dispersed in PBS buffer at ~0 min, 30 min and 60 min. Two concentrations at 100 μg ml^{-1} and 10 μg ml^{-1} are chosen for the two NP samples, respectively

Concentration/μg ml^{-1}	Duration/min	Hydrodynamic radius/nm
10	0	48
	30	29
	60	34
100	0	29, 182
	30	57, 279
	60	94, 1912

cells as an example, and then elaborate on subtle difference observed among different NPs and/or cell lines.

Dark contrast spherical shapes can be observed in the TEM images of the fixed cells after NPs' feeding. In Fig. 2, one can see these dark particles are mostly encapsulated by an organelle. Occasionally, a single particle has been observed in the cytoplasm (as indicated by the arrow in Fig. 2b), but particles have never been found in the nucleus for hundreds of cells examined by TEM. EDX taken from such particles and particle aggregates reveals their composition of Si and O. In the TEM, we could directly observe many NPs located either in membrane-bound organelles or in the cytoplasm after their being incubated with the H1299 cells. Such results are further confirmed by confocal microscopy (Fig. S2†), in which we have adopted 50 nm fluorescent amorphous silica NPs (dye doped for luminescence signals, corresponding DLS (Table S1†) and ζ potential measurements (Fig. S8†) could be found in the ESI†) in the cell feeding process with other experimental conditions kept the same. The punctated distribution of NPs indicates that the NPs are in aggregated form, most likely located in organelles. NPs have never been found in the nucleus (Fig. S2†).

We have also carried out the experiments to study the temperature effect on the cellular uptake of silica NPs. Two samples have been compared with one incubated at relatively low temperature (4 °C) and the other at normal human body temperature (37 °C). NPs can be easily observed in the TEM images taken from cells incubated at 37 °C (Fig. S3a†, image taken from a 3 hour incubated sample). As a comparison, the amount of NPs inside cell is significantly reduced after they are incubated at 4 °C (Fig. S3b†, image also taken from a 3 hour incubated sample).

To systematically study the interaction of NPs with the cells, we have incubated cells with NPs for different duration (3, 10, and 48 hours, respectively). At the end of each incubation period, cell samples have been collected for various analyses.

The entry process of NPs into the cells is illustrated in Fig. 3a–c (TEM images taken from a 3 hour incubated sample as a representative example). NPs have been found either outside the cell (being adhered to (Fig. 3a) or embraced (Fig. 3b) by the cell membrane), or inside the cells (being enclosed in vesicle-like organelles (Fig. 3c)). The evolution of the NP distribution inside the cell is disclosed by TEM images taken from samples of different incubation duration. Most of the NPs have been found in mono-dispersed form in endo-lysosomes or cytoplasm (Fig. 3d and e) after 3 hours incubation; as the incubation time is elongated to 10 hours and further to 48 hours, more and more clustering of multiple NPs appear in the endo-lysosomes (Fig. 3f and h), while very few single particles are found in the cytoplasm (Fig. 3g and i). The observation of a large amount of membrane bounded NPs inside the cells, together with the fact that no specific coating is deposited on the NP surface, suggest non-specific endocytosis as the major mechanism for the cellular uptake of the nanoparticles. The comparison made between samples incubated at relatively low (4 °C) and high (37 °C) temperatures also suggests the endocytosis is an energy dependent process. This is consistent with the literature report.[5]

Although bare NPs have also been found in the cytoplasm (Fig. 3g–i), the amount is small. It is possible that broken organelles can release the NPs to the cytoplasm. In fact, a partially ruptured organelle containing NPs has been observed (Fig. S4d†) in the NP-fed cells.

We have measured the ζ potential of the NPs as a function of the pH value (Fig. S8†), and found that the NP surface is negatively charged with a value of 30 mV in physiological environments such as that in early endosomes (pH ≈ 7). However, the nature of the surface charge would change to slightly positive, and a much smaller value of 4 mV, in an acidic environment such as that in lysosomes (pH ≈ 4).[31] It has been found by Panyam *et al.* that the electrostatic attraction between the positively charged nanoparticle surface and the negatively charged organelle membrane (such as endosome and lysosome) may induce organelle rupture.[31] In this sense, the SiO_2 NPs should be relatively stable in the early endosome and have a larger chance of being released to the cytoplasm when they reside in a lysosome due to its rupture. Nevertheless, even the lysosome rupture probability does not seem to be high as most of the nanoparticles still remain in the lysosomes and very few have been released to the cytoplasm, as suggested by the confocal microscopy results taken from lysotracker marked samples (Fig. S5†). In fact, nanoparticle escaping from endosome/lysosome involves complex chemistry,[32–34] and the explanation using electrostatic interaction only makes a partial contribution.

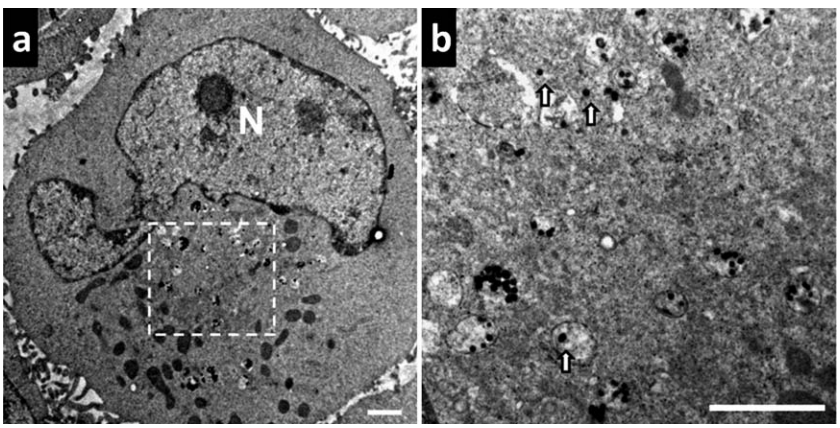

Fig. 2 (a) TEM image of one of the H1299 cells treated with 50 nm amorphous SiO_2 NPs; (b) magnified TEM image of selected region in (a). (The scale bar is 1 μm, N stands for "nucleus" in the cell.)

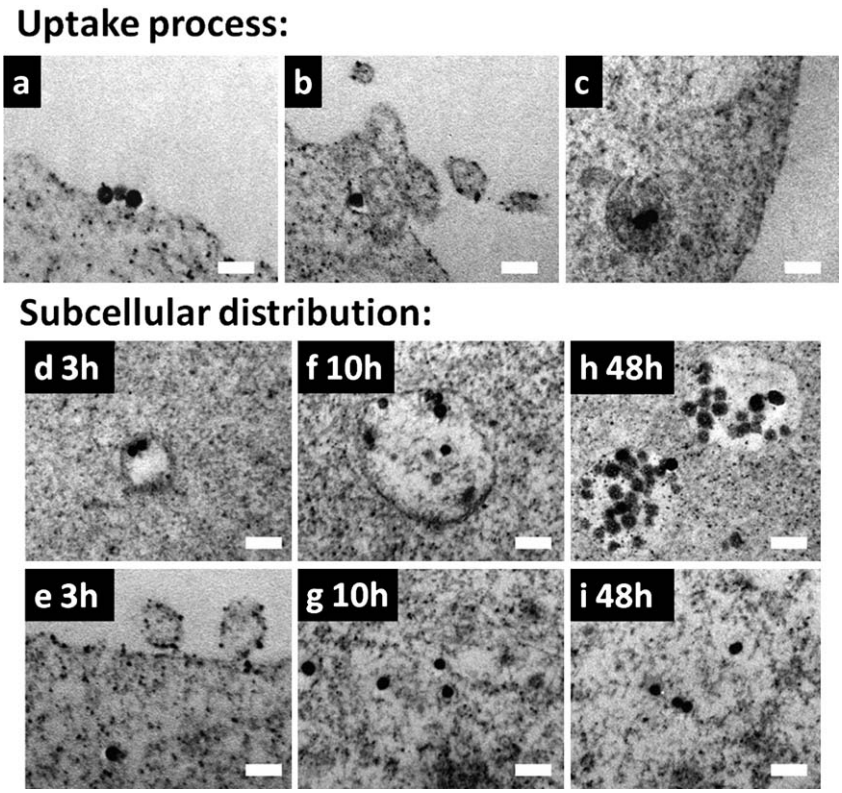

Fig. 3 TEM images disclosing the interaction between the 50 nm amorphous SiO_2 NPs and the H1299 cells; (a)–(c) describe the different stages of the endocytosis process; (d)–(i) show the typical distribution of the SiO_2 NPs within the H1299 cells as a function of the incubation duration: (d) and (e) 3 hours; (f) and (g) 10 hours; (h) and (i) 48 hours. (The scale bar is 100 nm.)

It is interesting to note that most of the NPs remain as monodispersed in the lysosomes for short incubation times (*e.g.* the 3 hours and 10 hours), and large organelles with NP clusters only become abundant at longer incubation duration (*e.g.* 48 hours). Such experimental results suggest the evolution of NPs once they are inside the cells, *i.e.*, small organelles containing NPs would join together and form larger ones, while the NPs aggregate inside the newly formed organelles. One should note that large NP concentrations during the feeding may cause NPs aggregation before they enter the cells. Nevertheless, both the DLS results and literature reports of similar systems[35] suggest it is not likely in the present study.

It is interesting to note that membrane-bound NPs are observed outside the cells during the feeding process (Fig. 4a–c, images taken from a 48 hour incubated sample), suggesting that NPs excretion from inside the cell occurs simultaneously with endocytosis.

The excretion of NPs is further confirmed by transferring the NP-fed cells to NP-free medium for 1 hour, and comparing the cell samples before and after the medium change. NPs (mostly in lysosomes) can be easily observed in the TEM images taken from particle-fed cells (Fig. 4d, image taken from a 48 hour incubated sample). As a comparison, the amount of NPs inside the cells is significantly reduced after they have been incubated in fresh, NP-free medium (Fig. 4e, image taken from the same sample after an additional 1 hour incubation in NP-free medium). Similar findings have been obtained using confocal microscopy, *i.e.*, the fluorescent intensity of the NPs decreases dramatically after the medium change (Fig. S6†).

The significant change observed in the 48 hour and 48 + 1 hour sample is mainly induced by the medium change. It is important to note that the endocytosis and exocytosis processes are dynamic and they take place simultaneously. The rates of both endocytosis and exocytosis are dependent on the amount of nanoparticles inside and outside the cells. That is to say, when the medium is changed to nanoparticle free, the huge difference between the amount of silica nanoparticles inside and outside the cells makes the excretion process dominant, which explains the corresponding TEM and confocal observation.

Interestingly we have also found that after an additional one hour incubation in the fresh, NP-free medium, most of the NP aggregates in the organelles disappear but with some single NP left in the cytoplasm (Fig. 4d and e). This finding suggests that NP clusters in lysosomes are more easily excreted by the cells when compared to the single NP in cytoplasm. In a typical exocytosis process, the NPs should firstly be wrapped by lysosomes before their delivery to the periphery of cells, where they fuse with the cell membrane to complete the excretion. In this sense, it is expected that an easy fusion between the lysosomes (with NPs inside) and the cell membrane should contribute the observed excretion difference.

2.2 Factors influencing the NP–cell interaction

2.2.1 The effect of serum (in the incubation medium) on cellular uptake. To find out how serum would affect the cellular uptake of the NPs, the cells have been treated respectively with 50 nm amorphous SiO_2 NPs in SFM, and SCM for 48 hours.

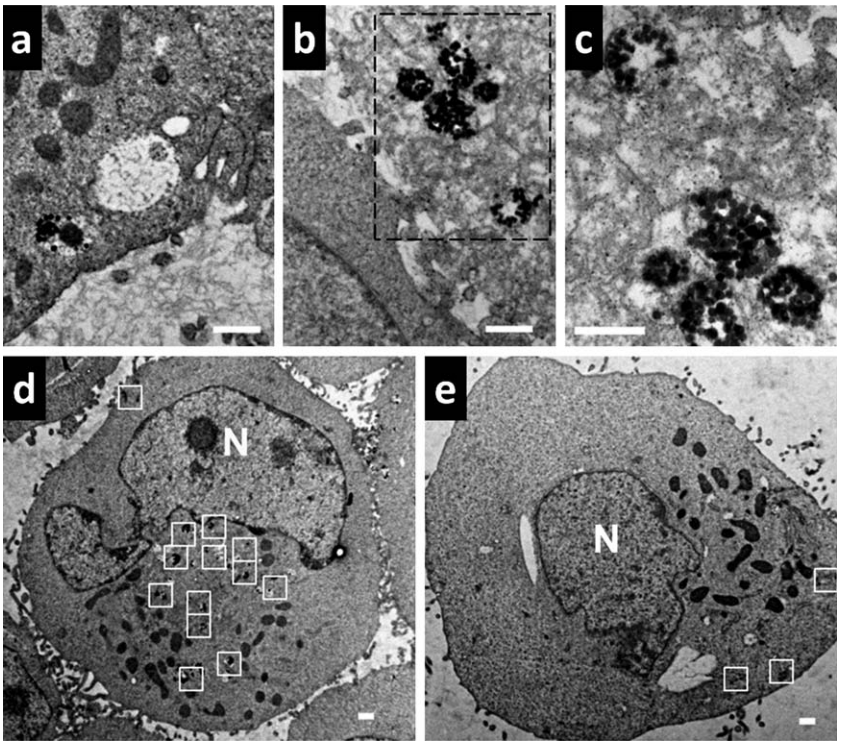

Fig. 4 TEM images suggesting the exocytosis of 50 nm amorphous SiO_2 NPs from the H1299 cells: (a) particle containing vesicle observed inside the cell close to the cell membrane; (b) particle containing vesicles observed outside the cell; (c) the magnified rectangle-marked area in (b), clearly showing that these vesicles are membrane bounded; (d) typical TEM image of H1299 cells treated with 50 nm amorphous SiO_2 NPs for 48 hours in serum free medium (SFM); (e) TEM image taken from the same sample after an additional one hour incubation in fresh, NP-free SFM. The white rectangle marked areas indicate the NPs' location. (The scale bar is 500 nm, N stands for "nucleus" in the cell.)

After incubation, NPs (mostly in lysosomes) can be easily observed in the cells incubated with NPs in SFM (Fig. 5a). As a comparison, the amount of NPs inside cells is much less when they are incubated with NPs in SCM (Fig. 5b). Similar phenomena have been observed in confocal microscopy, *i.e.*, the fluorescent intensity of the NPs is much weaker from the SCM incubated sample (Fig. S7†).

It has been reported that the serum in the medium would promote the cellular uptake of NPs in a number of different material systems, including Au,[5] cerium oxide,[36] and polymer NPs,[37,38] *etc.* This seems to contradict the observation in the present study. As a matter of fact, one needs to consider another effect brought by the serum introduction. Once the NPs are introduced to the biological system such as culture medium in the presence of serum, protein adsorption will affect the surface charge distribution of NPs and reduce its ζ potential.[39] Consequently, the NPs' agglomeration occurs much more easily due to their surface protein adsorption. As the size of the NP clusters becomes larger, cellular uptake can be difficult. In this sense, the two opposite effects brought by the serum would compete with

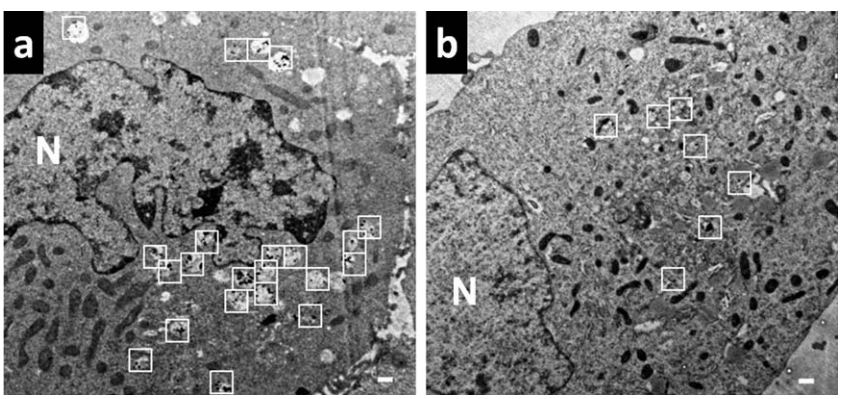

Fig. 5 Typical TEM images showing the serum effect on cellular uptake of the NPs: H1299 cells treated with 50 nm amorphous SiO_2 NPs for 48 hours (a) in SFM; and (b) in serum containing medium (SCM). (Rectangle marked areas indicate the location of NPs; the scale bar is 500 nm; N stands for "nucleus" in the cell.)

each other, and the overall endocytosis process could differ from case to case (depending on the NPs' surface properties).[36–38,40]

2.2.2 Crystallinity effect—distribution of amorphous and crystalline SiO_2 NPs in the cells. To find the difference between crystalline and amorphous NPs interacting with cells, crystalline fine silica particles with size ranging from several tens to hundreds of nanometres and ~400 nm amorphous silica NPs have been respectively chosen to incubate with cells in SFM for 48 hours. For crystalline particles, they could be easily observed in cytoplasm without being encapsulated by membrane (Fig. 6a, image taken from a 48 hour incubated sample), although lysosomes containing NPs also exist in the cells. As a comparison, amorphous silica NPs are always found in lysosomes (Fig. 6b, image taken from a 48 hour incubated sample). For hundreds of cells examined, we have found that crystalline fine particles have a much higher chance to be found in the cytoplasm, while the amorphous ones are mostly located in lysosomes. The existence of membrane bounded organelles containing crystalline silica particles basically supports the endocytosis process. As both types of NPs take endocytosis as the main pathway to enter the cell interior, they should stay in the organelles unless the membrane ruptures. Consequently, the observed difference in the distribution of the crystalline and the amorphous NPs suggests a higher probability for the former to rupture the organelle membrane inside the cells. In addition, the surface chemical characteristics are found to be different for the two types of NPs. The ζ potential of crystalline silica particles as a function of the pH value shows that its value is larger than that of the amorphous ones in the range of pH value from 4–6 (Fig. S8†), indicating that the surface of the crystalline NPs is more charged at such conditions. Such a difference may partially contribute to the easier lysosome rupture as observed in the crystalline NPs-fed cell samples.[34]

2.3 Factors affecting the exocytosis process. Although similar results are found in different cell lines regarding the NP endocytosis and distribution/evolution inside the cells, the cell line difference seems to affect the exocytosis process. In the normal cell line NE083, the excretion of NPs appears to be much slower than that of H1299 cells (and other cell lines examined). Similar experiments have been conducted by comparing the NE083 cell samples before and after the medium change (from NP-containing to NP-free). NPs (mostly in lysosomes) could be easily observed in the TEM images taken from NP-fed NE083 cells (Fig. 7a, image taken from a 48 hour incubated sample). Only a slight decrease in the NPs amount could be observed after they have been further incubated in fresh NP-free medium for one hour (Fig. 7b, image taken from the same sample after an additional 1 hour incubation in NP-free medium). An obvious decrease in the amount of NPs can only be observed after another two hours incubation (Fig. 7c, image taken from the same sample after an additional 3 hours incubation in NP-free medium). This is quite different from that obtained from the H1299 cells (also from NL 20 cells)—the amount of NPs inside these cells is significantly reduced after they are incubated in fresh NP-free medium for only 1 hour (Fig. 4d and e). The observed difference in the secreting NPs by different cells suggests that this process is time dependent.

3. Cytotoxic effect of silica NPs on cells

Both the H1299 and NE083 cells have been treated with silica NPs at 0.156, 0.313, 0.625, 1.25, 2.5, 5 and 10 μg ml^{-1} dosage levels for 24, and 48 hours. The MTT assay results are shown in Fig. 8. For 50 nm amorphous silica NPs, no significant decrease in the cell viability (mostly >90%) could be observed with increasing particle concentration for either 24 hours or 48 hours incubation (Fig. 8a and b), for both cell lines alike. Consistent observations have been made from light microscopy—no obvious cell morphology change has been found after their being incubated with the NPs (Fig. S10†). Similar results have been obtained for both larger (400 nm) and smaller (10–20 nm) sized amorphous silica NPs, *i.e.*, the decrease of cell viability is negligible (Fig. S9†). However, the crystalline fine silica particles seem to have much different impact on the cells. Although the decrease of cell viability is negligible (mostly >90% of control) at low NP concentrations (<2.5 μg ml^{-1}) even after 48 hours incubation, the cell viability decreases to a level of ~60% to 80% at higher NPs concentrations (>5 μg ml^{-1}) after similar incubation duration

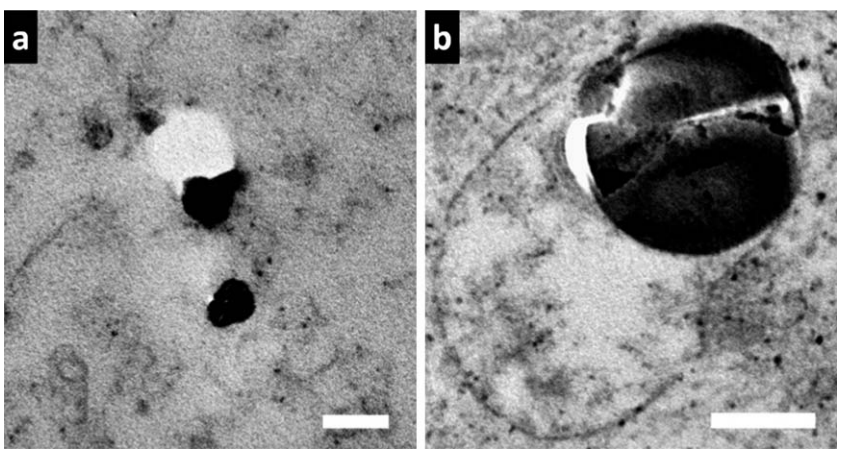

Fig. 6 TEM images showing (a) crystalline silica fine particles in cytoplasm; and (b) 400 nm amorphous silica NPs in a lysosome inside the H1299 cells. (The scale bar is 200 nm.)

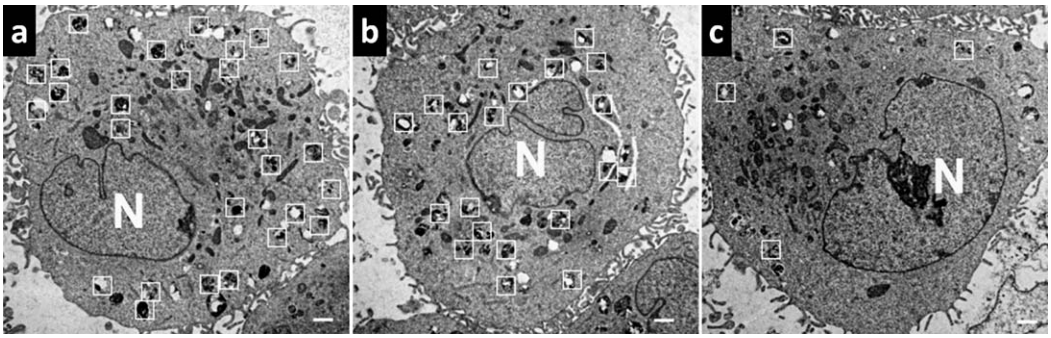

Fig. 7 TEM images of NE083 cells treated with 50 nm SiO_2 NPs for (a) 48 hours in SFM; TEM image taken from the same sample after (b), an additional 1 hour and (c), 3 hours incubation in fresh and NP-free SFM. (Rectangle marked areas indicate the location of NPs; the scale bar is 1 μm; N stands for "nucleus" in the cell.)

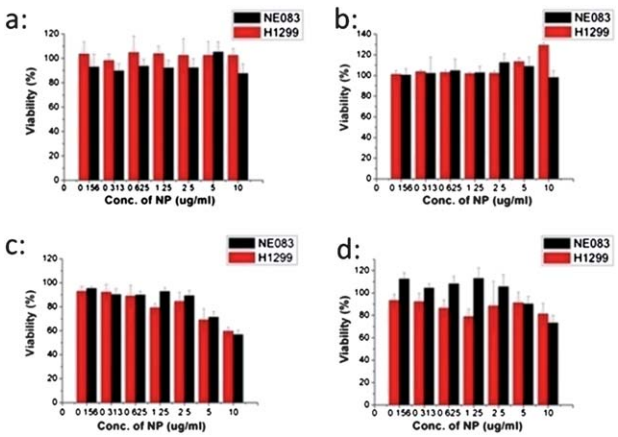

Fig. 8 Cytotoxicity of silica NPs on H1299 cells and NE083 cells after 24 hours and 48 hours incubation. Cell incubated with the 50 nm amorphous NPs for (a), 24 hours and (b), 48 hours; cell incubated with crystalline fine silica particles for (c), 24 hours and (d), 48 hours. Data are presented with mean ± standard deviation (SD) from four independent experiments. Significance indicated by $p < 0.05$, analyzed by student's t test.

(Fig. 8c and d). A number of other cell lines (NL20, HEK293 and HONE1) have also been tested under the same experimental conditions, and similar viability results have been obtained.

In our study, little cytotoxicity effect is identified for amorphous silica NPs at low concentration range (<2.5 μg ml^{-1}). This finding is consistent with the previous report on the cytotoxicity of amorphous silica NPs at low dose.[8–11,13,39] However, it has been found in the literature[8–11,13,41] that increased cytotoxicity appears at high NP dose and/or elongated incubation duration. In this sense, the observed low cytotoxicity in the present study can be ascribed to the cell capability of NP excretion, as well as the fact that NPs are captured inside lysosomes, being relatively isolated from the interior of the cell.

When comparing the effect of amorphous and crystalline silica particles *in vitro*, the amorphous particles show less cytotoxicity than the crystalline ones.[42] This is also observed in the present study, *i.e.*, the crystalline silica nanoparticles are more likely to rupture the organelle membrane, leading to direct contact between the nanoparticle and the cytoplasm, and thus direct chemical exchange, which may affect the cell's regular functioning. As discussed in earlier sections, the crystalline NPs may easily rupture the lysosome membrane due to their unique physiochemical property.[28,43,44] Their irregular morphology, more reactive surface, and higher potential to generate reactive oxygen species (ROS)[28] all contribute to the observed phenomenon.

Conclusions

We have identified non-specific endocytosis as the major mechanism for cellular uptake of the SiO_2 NPs, which is consistent with most of the reported mechanisms of NP uptake. In a non-specific endocytosis process, serum in the medium does not necessarily promote that NP cellular uptake process, as it increases NPs' aggregation. The direct consequence of endocytosis is the formation of membrane bound organelles (containing NPs) inside the cells. These organelles are fairly stable against rupture, as very few NPs have been found to be released into the cytoplasm. Ruptured organelles have been observed, which is more frequent in crystalline NPs-fed cell samples than in the amorphous case. Fusing of the organelles and aggregation of the NPs are found inside the cells, suggesting the dynamic nature of the NP–cell interaction. The excretion of the NPs (*via* exocytosis) occurs simultaneously with the uptake process. The amount of NPs inside the cell is dependent on the amount of NPs outside cells in the medium. Obvious cytotoxicity is not observed for both amorphous and crystalline SiO_2 NPs at low NP dose (<2.5 μg ml^{-1}), being generally consistent with the literature.

Experimental section

1. Preparation of silica NPs

Two different types of silica NPs, *i.e.*, amorphous and crystalline, are selected in the present study.

The amorphous silica NPs were synthesized using the standard Stober's method,[45] which produces spherical NPs with controllable size and rather narrow size distribution. Nevertheless, such a method fails to produce NPs with size smaller than 20 nm.[45] In order to investigate the size effect on the possible interactions between the amorphous NPs and the cells, we therefore adopted NPs with larger diameters (400 nm and 50 nm in diameter) synthesized by Stober's method and smaller ones (10–20 nm in diameter) purchased from Sigma. Commercial fluorescent amorphous silica NPs with 50 nm diameter (Ex/Em: 569/585 nm;

Kisker, Germany) were employed for confocal microscopy study.

The crystalline silica NPs were purchased from Sigma. Centrifugation was applied to the purchased crystalline NPs in order to reduce its size distribution. In a typical procedure, 500 mg NP powder is dissolved in 7 ml ethanol and sonicated for 10 minutes. Centrifugation is carried out at 3000 rpm for 10 minutes. The supernatant is then taken out and centrifuged again at 10 000 rpm for another 10 minutes. At last, white precipitate is dried in vacuum at 200 °C for further use.

2. Basic characterizations of the NPs

The general morphology, size, and the size distribution of the NPs were characterized using transmission electron microscopy (TEM, PhilipsCM120). The chemical composition of the silica NPs was investigated by X-ray Photoelectron Spectrometer (XPS) (PHI Quantum 2000). The surface of the silica NPs was studied by Fourier Transform Infrared Spectrometer (FTIR; Nicolet 670, Thomas Nicolet, Waltham, MA).

Dynamic light scattering (DLS) was used to study the stability of silica NP in solution as a function of time. This is rather important, as aggregation of NPs would directly affect the NP–cell interaction. The DLS spectrum of silica NPs in PBS buffer solution was measured. The measurable angle was fixed at 20°. The average ζ potential of the silica NPs under an electric field in aqueous solution was measured using a commercial zeta potential spectrometer (ZetaPlus, Brookhaven) with two platinum-coated electrodes. A He–Ne laser (output power 28 mW at 632.8 nm) was used as the light source. All measurements were carried out at room temperature (25 °C).

3. Study of the interaction of silica NPs with human cells

3.1 Cell culture. Several lines including H1299 human lung carcinoma cell, HONE1 human nasopharyngeal carcinoma cell, NE083 human esophageal epithelial cell, NL20 human bronchial epithelial cell and HEK293 human embryonic kidney cell were used in this study. The H1299 and HONE1 cell were cultured in RPMI 1640 medium while NE083, NL20 and HEK293 cell were cultured in Dulbecco's modified Eagle's medium (DMEM) with or without fetal bovine serum (10%). All medium contains 1% streptomycin and 1% penicillin. All cells were cultured at 37 °C in a water-saturated incubator with 5% CO_2.

3.2 Introducing NPs to cell culture. All the NPs were sterilized before use by either steaming at 115 °C (NPs in powder form) for 2 hours or syringe filtering with a pore size of 0.22 μm (NPs in solution). The final NPs were dispersed in the medium by ultrasonication for at least 30 minutes right before their introduction to the cells. Cells were seeded at initial densities of 5×10^4 cells per ml in flask and incubated for 24 hours before introducing NPs, after that the original NP-free medium was discarded and the fresh prepared NP-containing medium was added with different NP concentrations. Different cell "feeding time" was adopted, as specified in individual experimental results.

For endocytosis study, both H1299 and NE083 cells were fed with 10 μg ml^{-1} of silica NPs (both amorphous or crystalline) for different duration (3 hours, 10 hours, 24 hours, 48 hours) in SCM or SFM as described above.

For exocytosis study, H1299, NL20 and NE083 cells were fed with 10 μg ml^{-1} of 50 nm amorphous silica NPs in SFM. After 48 hours incubation, the cells were washed with PBS buffer for three times and then incubated with fresh, NP-free SFM for another one hour or three hours.

3.3 TEM study on NPs–cell interaction. The NP-fed cells were washed with PBS buffer three times and then fixed with 2.5% glutaraldehyde at 4 °C for 12 hours, before they were post-fixed in 1% osmium tetraoxide for 1 hour at room temperature. After that, the cells were washed with PBS and embedded into 2% agar cube. The cell cube were dehydrated in ethanol of increasing concentration (50%, 70%, 90% and 100%) in a sequential manner and lastly with propylene oxide. Microtome (Leica, EM UC6) was then used to cut the cured cell cube (in Spurr resin (Electron microscopy sciences, USA)) into thin slices (70–90 nm in thickness). The samples were collected on 300 mesh copper grids and double stained with 2% aqueous uranyl acetate and commercial lead citrate aqueous solution (Leica).

3.4 Confocal microscopy study on NPs–cell interaction. The confocal microscopy has been carried out on both fixed and live cells. For fixed cells, the NP-fed cells were fixed with 2.5% glutaraldehyde at room temperature for 10 minutes, then the cell samples were observed using confocal laser scanning microscopy (TCSP5, Leica) with a 63× water-immersion objective lens.

4. Evaluating the cytotoxicity of NPs by MTT assay

Cells were seeded in 96-well microtiter plates at initial densities of 5000 cells per well in serum free medium (100 μl). After allowing 24 hours for cell attachment, original medium was discarded and the silica NP-containing medium with different NP concentrations (0.156 μg ml^{-1} to 10 μg ml^{-1}) was added (150 μl) to the cell samples. The cells were incubated in the NP-containing medium for different duration. Cytotoxic effect was then evaluated using MTT assay.[46] Briefly, the original medium was removed, and fresh NP-free medium containing MTT salt (1 : 10 dilution) was added and the cells were further incubated (37 °C, 5% CO_2) for 4 hours. After carefully removing the medium, the purple formazan formed in the cells was dissolved in dimethylsulfoxide. The absorbance of formazan at 570 nm with a reference of 690 nm was determined by a spectrophotometer. Cell viability was calculated as a percentage compared to control samples (treated without NPs).

Acknowledgements

The authors are grateful to Mr Z. F. Li for DLS measurements and Prof. C. Wu for stimulating discussions. This work is supported by grants from RGC of HKSAR under project no. 414709, 414710, and NSFC (10928408).

References

1 L. Latterini and M. Amelia, *Langmuir*, 2009, **25**, 4767–4773.
2 H. L. Tu, Y. S. Lin, H. Y. Lin, Y. Hung, L. W. Lo, Y. F. Chen and C. Y. Mou, *Adv. Mater.*, 2009, **21**, 172–177.

3 V. Vijayanathan, T. Thomas and T. J. Thomas, *Biochemistry*, 2002, **41**, 14085–14094.
4 B. Z. Zhao, J. J. Yin, P. J. Bilski, C. F. Chignell, J. E. Roberts and Y. Y. He, *Toxicol. Appl. Pharmacol.*, 2009, **241**, 163–172.
5 B. D. Chithrani and W. C. W. Chan, *Nano Lett.*, 2007, **7**, 1542–1550.
6 B. D. Chithrani, A. A. Ghazani and W. C. W. Chan, *Nano Lett.*, 2006, **6**, 662–668.
7 D. B. Chithrani, M. Dunne, J. Stewart, C. Allen and D. A. Jaffray, *Nanomed.: Nanotechnol. Biol. Med.*, 2010, **6**, 161–169.
8 T. J. Brunner, P. Wick, P. Manser, P. Spohn, R. N. Grass, L. K. Limbach, A. Bruinink and W. J. Stark, *Environ. Sci. Technol.*, 2006, **40**, 4374–4381.
9 J. S. Chang, K. L. B. Chang, D. F. Hwang and Z. L. Kong, *Environ. Sci. Technol.*, 2007, **41**, 2064–2068.
10 M. Chen and A. von Mikecz, *Exp. Cell Res.*, 2005, **305**, 51–62.
11 W. S. Lin, Y. W. Huang, X. D. Zhou and Y. F. Ma, *Toxicol. Appl. Pharmacol.*, 2006, **217**, 252–259.
12 D. Napierska, L. C. J. Thomassen, V. Rabolli, D. Lison, L. Gonzalez, M. Kirsch-Volders, J. A. Martens and P. H. Hoet, *Small*, 2009, **5**, 846–853.
13 R. Wottrich, S. Diabate and H. F. Krug, *Int. J. Hyg. Environ. Health*, 2004, **207**, 353–361.
14 J. Xie, C. Xu, N. Kohler, Y. Hou and S. Sun, *Adv. Mater.*, 2007, **19**, 3163–3166.
15 T. Xia, M. Kovochich, M. Liong, L. Madler, B. Gilbert, H. B. Shi, J. I. Yeh, J. I. Zink and A. E. Nel, *ACS Nano*, 2008, **2**, 2121–2134.
16 S. J. Cho, D. Maysinger, M. Jain, B. Roder, S. Hackbarth and F. M. Winnik, *Langmuir*, 2007, **23**, 1974–1980.
17 C. Kirchner, T. Liedl, S. Kudera, T. Pellegrino, A. M. Javier, H. E. Gaub, S. Stolzle, N. Fertig and W. J. Parak, *Nano Lett.*, 2005, **5**, 331–338.
18 J. O. Winter, T. Y. Liu, B. A. Korgel and C. E. Schmidt, *Adv. Mater.*, 2001, **13**, 1673–1677.
19 K. Kostarelos, L. Lacerda, G. Pastorin, W. Wu, S. Wieckowski, J. Luangsivilay, S. Godefroy, D. Pantarotto, J. P. Briand, S. Muller, M. Prato and A. Bianco, *Nat. Nanotechnol.*, 2007, **2**, 108–113.
20 S. Foley, C. Crowley, M. Smaihi, C. Bonfils, B. F. Erlanger, P. Seta and C. Larroque, *Biochem. Biophys. Res. Commun.*, 2002, **294**, 116–119.
21 J. K. Vasir and V. Labhasetwar, *Biomaterials*, 2008, **29**, 4244–4252.
22 A. Verma and F. Stellacci, *Small*, 2010, **6**, 12–21.
23 L. Wang, Y. Liu, W. Li, X. Jiang, Y. Ji, X. Wu, L. Xu, Y. Qiu, K. Zhao, T. Wei, Y. Li, Y. Zhao and C. Chen, *Nano Lett.*, 2011, **11**, 772–780.
24 H. Jin, D. A. Heller and M. S. Strano, *Nano Lett.*, 2008, **8**, 1577–1585.
25 J. Panyam and V. Labhasetwar, *Pharm. Res.*, 2003, **20**, 212–220.
26 N. Lewinski, V. Colvin and R. Drezek, *Small*, 2008, **4**, 26–49.
27 K. O. Yu, C. M. Grabinski, A. M. Schrand, R. C. Murdock, W. Wang, B. H. Gu, J. J. Schlager and S. M. Hussain, *J. Nanopart. Res.*, 2009, **11**, 15–24.
28 M. Ghiazza, M. Polimeni, I. Fenoglio, E. Gazzano, D. Ghigo and B. Fubini, *Chem. Res. Toxicol.*, 2010, **23**, 620–629.
29 B. Saikia, G. Parthasarathy and N. Sarmah, *Bull. Mater. Sci.*, 2008, **31**, 775–779.
30 T. Ngai, X. C. Xing and F. Jin, *Langmuir*, 2008, **24**, 13912–13917.
31 J. Panyam, W. Z. Zhou, S. Prabha, S. K. Sahoo and V. Labhasetwar, *FASEB J.*, 2002, **16**, 1217–1226.
32 W. T. Godbey, M. A. Barry, P. Saggau, K. K. Wu and A. G. Mikos, *J. Biomed. Mater. Res.*, 2000, **51**, 321–328.
33 A. Remy-Kristensen, J. P. Clamme, C. Vuilleumier, J. G. Kuhry and Y. Mely, *Biochim. Biophys. Acta, Biomembr.*, 2001, **1514**, 21–32.
34 I. Slowing, B. G. Trewyn and V. S. Y. Lin, *J. Am. Chem. Soc.*, 2006, **128**, 14792–14793.
35 D. Lison, L. C. J. Thomassen, V. Rabolli, L. Gonzalez, D. Napierska, J. W. Seo, M. Kirsch-Volders, P. Hoet, C. E. A. Kirschhock and J. A. Martens, *Toxicol. Sci.*, 2008, **104**, 155–162.
36 S. Patil, A. Sandberg, E. Heckert, W. Self and S. Seal, *Biomaterials*, 2007, **28**, 4600–4607.
37 S. Nagayama, K. Ogawara, Y. Fukuoka, K. Higaki and T. Kimura, *Int. J. Pharm.*, 2007, **342**, 215–221.
38 S. Nagayama, K. Ogawara, K. Minato, Y. Fukuoka, Y. Takakura, M. Hashida, K. Higaki and T. Kimura, *Int. J. Pharm.*, 2007, **329**, 192–198.
39 L. K. Limbach, Y. C. Li, R. N. Grass, T. J. Brunner, M. A. Hintermann, M. Muller, D. Gunther and W. J. Stark, *Environ. Sci. Technol.*, 2005, **39**, 9370–9376.
40 D. E. Owens and N. A. Peppas, *Int. J. Pharm.*, 2006, **307**, 93–102.
41 N. Li, C. Sioutas, A. Cho, D. Schmitz, C. Misra, J. Sempf, M. Y. Wang, T. Oberley, J. Froines and A. Nel, *Environ. Health Perspect.*, 2003, **111**, 455–460.
42 D. B. Warheit, T. A. McHugh and M. A. Hartsky, *Scand. J. Work, Environ. Health*, 1995, **21**, 19–21.
43 S. Linder and M. C. Shoshan, *Drug Resist. Updates*, 2005, **8**, 199–204.
44 Y. Zhu, W. X. Li, Q. N. Li, Y. G. Li, Y. F. Li, X. Y. Zhang and Q. Huang, *Carbon*, 2009, **47**, 1351–1358.
45 W. Stober, A. Fink and E. Bohn, *J. Colloid Interface Sci.*, 1968, **26**, 62–69.
46 T. Mosmann, *J. Immunol. Methods*, 1983, **65**, 55–63.